COMPRESSIVE SENSING FOR SYNTHETIC APERTURE IMAGING USING A SPARSE BASIS TRANSFORM

Christian Debes

AGT Group (R&D) GmbH
Darmstadt, Germany

Stefan Leier, Fabio Nikolay and Abdelhak M. Zoubir

Signal Processing Group, Technische Universität Darmstadt
Darmstadt, Germany

1. ABSTRACT

We consider the problem of active high-resolution imaging using synthetic aperture techniques, such as synthetic aperture radar (SAR) or synthetic aperture sonar (SAS). In order to reduce storage, processing power and energy requirements a compressive sensing framework is adopted that allows to reduce the number of measurements while maintaining range resolution and image quality. We consider the approach from Alonso *et al.* where compressive sensing is considered as an alternative to matched filtering for range focusing while keeping along-track focusing for imaging unmodified. This approach is extended by a sparse basis transform for range profiles that allows for deviations from the implicit point target model assumption. A synthetic aperture ultrasound imaging system is build that implements the presented techniques in a laboratory setup. Range profiles and images of this setup are considered to evaluate the system performance in terms of resolution and image quality.

2. MOTIVATION

In order to overcome the limitations of real aperture imaging systems, namely the degradation of the along-track resolution with increasing range, synthetic aperture imaging systems [1] "synthetize" the effect of a large aperture by extending its length according to the focusing range. This concept is illustrated in Figure 1, where a small physical aperture, e.g. a transceiver, moves along a rectilinear path.

Classically, a matched filter is used at every receiver position for range focusing. An imaging algorithm for along-track focusing, such as the backprojection algorithm, is then applied to align the set of range profiles and form an image. Synthetic aperture systems typically have strong requirements in terms of processing power, data storage and energy, especially when considering autonomous vehicles. Reducing the number of needed measurement to form a range profile or an image is, thus, of high practical importance.

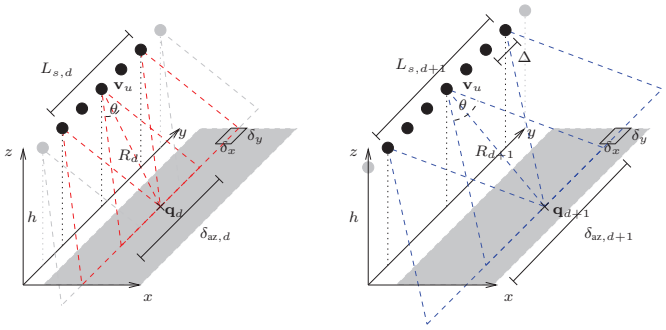

Fig. 1. Principle of a synthetic aperture imaging system

The theory of Compressive Sensing (CS) [2] allows to undersample signals given that they have a sparse representation in some domain, e.g. using the discrete cosine transform (DCT). CS has been successfully applied in numerous imaging applications such as optical imaging [3], Through-the-Wall Radar Imaging [4], to mention a few. Recently, Alonso *et al.* presented a CS framework for SAR [5] where range focusing is formulated as a CS optimization problem.

In this paper, we generalize the approach in [5] allowing for non-sparse range profiles which occur in practice due to extended and weak targets. We further demonstrate a practical implementation of the proposed CS-SAR using a synthetic aperture ultrasound system in a laboratory setup and evaluate its performance.

3. SYNTHETIC APERTURE DATA MODEL

Consider the notation as in Figure 1 where a synthetic array of larger size is formed through transmitting pulses and receiving at each element position u, with $u = 0, \ldots, M_u - 1$ the respective echoes $\mathbf{v}_u = [0, u \cdot \Delta, h]^T$, where h is the height and Δ the advance per ping of the imaging platform, respectively. Given a directivity of the transceiver θ, the physical footprint, $\delta_{\text{az},d+1} > \delta_{\text{az},d}$, increases for far off targets compared to nearby ones with $R_{d+1} > R_d$. Consequently, the synthetic aperture size increases, i.e. $L_{s,d+1} > L_{s,d}$, and therefore more observations are collected. This allows to form more narrow beams which yields the same along-track resolution δ_y for both slant-range distances, R_d and R_{d+1}. Note that in general the range resolution δ_x solely depends on the transmitted signal.

Consider a set of D stationary point targets each with a target reflectivity σ_d with $d = 1, ..., D$ that are located at positions $\mathbf{q}_d = [x_d, y_d, 0]^T$ within a finite two-dimensional scene of interest. To simplify matters, the reflectivity is assumed to be independent of frequency and angle of incidence. Moreover, any spreading losses and transmit and receive patterns are incorporated into σ_d. Then, the ideal target reflectivity function [6] of the scene of interest is

$$f(x, y) = \sum_{d=1}^{D} \sigma_d \delta(x - x_d, y - y_d). \tag{1}$$

Let the distance between the d^{th} target and the imaging platform at position $\mathbf{v}_u$ be denoted by $r_d(u) = \|\mathbf{q}_d - \mathbf{v}_u\|_{\ell_2}$. Subsequently, the echo signals can be expressed as the superposition of the individual target responses as

$$e(u, n) = \sum_{d=1}^{D} \sigma_d \cdot p\left(n - r_d(u) \cdot \frac{2}{cT_s}\right) \tag{2}$$

where $u = 0, \ldots, M_u - 1$, $n = 0, \ldots, M_n - 1$ with u and n denoting the slow- and fast-time, respectively. The speed of propagation of the wave in the respective medium is denoted as c, T_s the sampling rate and $p(n)$ the transmitted pulse form. An example of synthetic data measurements is shown in Figure 2(a) in the case of a linear frequency modulated pulse.

4. SYNTHETIC APERTURE IMAGING USING MATCHED FILTERING

Given the echo signals as in Equation (2), the objective of any synthetic aperture imaging algorithm is to focus the data in both dimensions - range and along-track - to obtain an image of the scene of interest or in other words, to get an estimate of $f(x, y)$. After demodulation, the base-band converted raw data, $e_{\text{LP}}(u, n)$, is first match-filtered to obtain the range focused or pulse-compressed signal as

$$e_{\text{MF}}(u, n) = e_{\text{LP}}(u, n) \circledast_n p^*(-n), \tag{3}$$

where $\circledast_n$ and * denotes convolution in time and complex conjugation, respectively. Figure 2(b) illustrates the outcome of the matched filter operation. While range focusing is achieved via matched filtering by almost all imaging techniques, they differ in the manner in which along-track focusing is performed. Here, we concentrate on the back-projection algorithm [6]. Let $\mathbf{g}_{kl} = [x_k, y_l, 0]^T$ with $k = 1, \ldots, N_x$ and $l = 1, \ldots, N_y$ be all points in the reconstruction grid of the scene, then the discrete focusing delay between the imaging platform and the grid point is $\tau_{kl}^{\text{foc}}(u) = 2 \cdot \|\mathbf{g}_{kl} - \mathbf{v}_u\|_2 / (cT_s)$ and an estimate of the reflectivity of

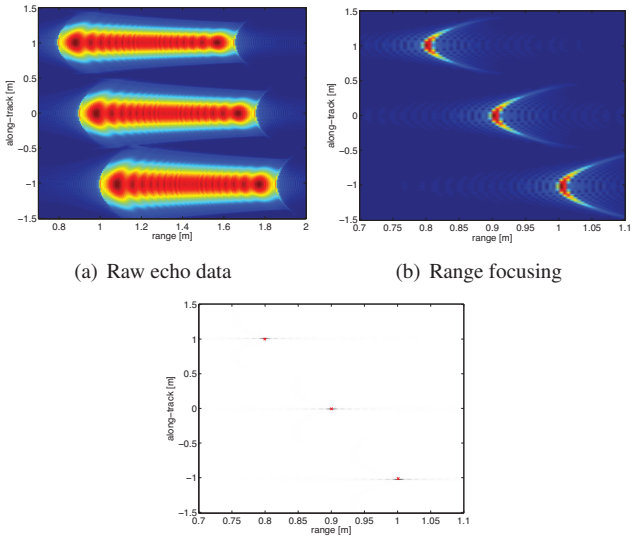

(a) Raw echo data (b) Range focusing

(c) Synthetic aperture image

Fig. 2. Illustration of range and along-track focusing in synthetic aperture imaging

the target scene is obtained by

$$\hat{f}(x_k, y_l) = \sum_{u=1}^{M_u} e_{\text{MF}}\left(u, \tau_{kl}^{\text{foc}}(u)\right) e^{j\omega_c \tau_{kl}^{\text{foc}}(u)} \tag{4}$$

with $k = 1, \ldots, N_x$ and $l = 1, \ldots, N_y$ where ω_c is the carrier frequency. Note that Equation (4) requires an interpolation. The outcome for focusing the pulse-compressed data in along-track is exemplarily shown in Figure 2(c).

5. SYNTHETIC APERTURE IMAGING USING COMPRESSIVE SENSING

Consider a single range profile at $u = u_0$ as per Equation (2) it can be rewritten in matrix notation as

$$\mathbf{e} = \mathbf{P}\boldsymbol{\sigma} + \boldsymbol{\eta} \tag{5}$$

where $\mathbf{P}$ is a matrix with shifted versions of the discretized pulse forms, e.g. chirp signals, and $\boldsymbol{\sigma}$ denotes the vectorized target reflectivities along the range profile. Further, we included an additive noise component $\boldsymbol{\eta}$ which in the following is assumed to be i.i.d. zero-mean Gaussian distributed. Using a CS framework as in [5] a random extraction matrix $\mathbf{R}$ can be used to undersample the acquired data as

$$\mathbf{e}_{\mathbf{CS}} = \mathbf{R}(\mathbf{P}\boldsymbol{\sigma} + \boldsymbol{\eta}) = \mathbf{R}\mathbf{P}\boldsymbol{\sigma} + \tilde{\boldsymbol{\eta}} \tag{6}$$

where $\tilde{\boldsymbol{\eta}}$ is the undersampled version of $\boldsymbol{\eta}$, following the same distribution. Let us now assume that a sparsifying linear transform $\boldsymbol{\Psi}$, such as the DCT, can be found such that $\boldsymbol{\sigma} = \boldsymbol{\Psi}\mathbf{s}$ where $\mathbf{s}$ has only few non-zero entries. Note that in [5], $\boldsymbol{\Psi} = \mathbf{I}$ was implicitly considered, meaning that the range profile itself was assumed to be sparse.

Given the final CS data model as $\mathbf{e}_{\mathbf{CS}} = \mathbf{R}\mathbf{P}\boldsymbol{\Psi}\mathbf{s} + \tilde{\boldsymbol{\eta}}$ an ℓ_1 minimization can be performed as

$$\hat{\mathbf{s}} = \arg\min_{\mathbf{s}} \|\mathbf{s}\|_{\ell_1} \tag{7}$$

Reformulated as a basic pursuit denoising problem

$$\hat{\mathbf{s}} = \arg\min_{\mathbf{s}} \left\{\|\mathbf{s}\|_{\ell_1} + \tau\|\mathbf{e}_{\mathbf{CS}} - \mathbf{R}\mathbf{P}\boldsymbol{\Psi}\mathbf{s}\|_{\ell_2}\right\} \tag{8}$$

it can be solved using e.g. the SpaRSA algorithm [7]. Here, τ is the regularization parameter, performing the trade-off between sparsity (ℓ_1-minimization of $\mathbf{s}$) and fit to the data (ℓ_2-minimization of the residuals). Given the estimate for $\mathbf{s}$ the range profile is finally obtained as $\hat{\boldsymbol{\sigma}} = \boldsymbol{\Psi}\hat{\mathbf{s}}$.

Note that by solving Equation (8) instead of Equation (3) only the range focusing part is changed. The along-track focusing, e.g. as per Equation (4) remains unchanged.

6. EXPERIMENTAL RESULTS

To validate the CS framework for SAR we consider the experimental setup in Figure 3 where a sensor platform is moving along a 3 m metallic rail, driven by a motor at a velocity of $v = 10$ cm/s. On the sensor platform one ultrasound transmitter and three receivers are mounted as a uniform linear array. The transmitter operates at a carrier frequency of $f_c = 40$ kHz and emits linear frequency modulated pulses of bandwidth $B = 4$ kHz with a duration $T_p = 10$ ms at a repetition rate of $T_i = 40$ ms. The sampling frequency in the baseband is set to $f_s = 10$ kHz which is 25% above the Nyquist rate.

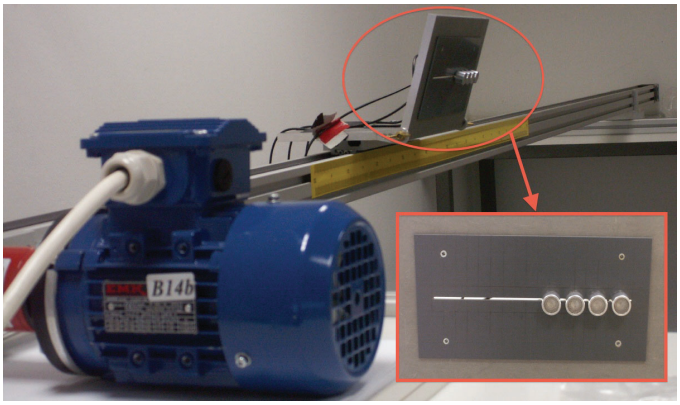

Fig. 3. Synthetic aperture imaging system

The first experimental setup to test range focusing capabilities consists of three six-pin integrated circuits (ICs) that are placed behind each other in range direction. For range focusing three techniques are considered: Classical matched filtering using 100% of the samples, CS without a SBT as proposed in [5] using 20% of the measurements and CS with the DCT as sparse basis using 20% of the measurements.

The output of range focusing for target distances of 6 and 12 cm using the three techniques are depicted in Figure 4. When considering a target distance of 12 cm (Figure 4(a)) both CS methods can resolve the three targets. As expected, CS without SBT shows a sparse range profile whereas the

proposed method using the DCT approaches the MF result. When reducing the target distance to 6 cm (Figure 4(b)) the advantages of using $\Psi = \mathbf{I}$, i.e. the assumption of a sparse range profile can be seen. In this case the three targets can still be resolved whereas CS with SBT and classical MF fail.

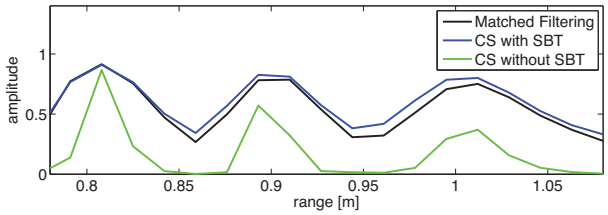

(a) Target distance: 12cm

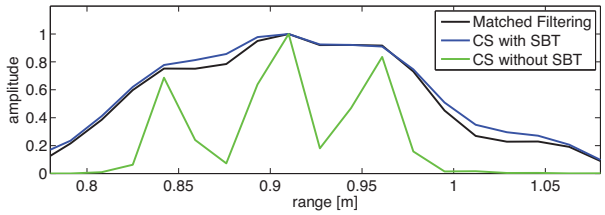

(b) Target distance: 6cm

Fig. 4. Range profiles using MF and CS

We now consider a scenario in which 95% of the measurements are discarded for estimating the range profile. Again, three ICs with target distance 12 cm are used. As shown in Figure 5, MF with only 5% of the measurements introduces strong aliasing effects. CS without SBT yields the zero solution whereas CS with SBT is still able to resolve all targets.

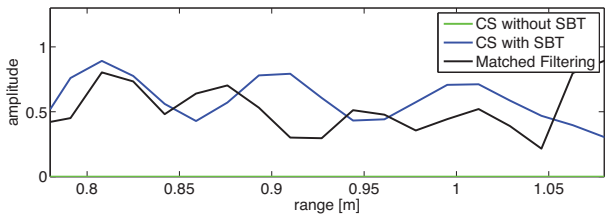

Fig. 5. Range profiles with only 5% of the measurements

The third experimental setup consists of the letters GRS placed one a table using metal nuts (Figure 6(a)). The back-projection algorithm as per Equation (4) is performed after range focusing. The resulting images are depicted in Figure 6 for MF as well as the two CS methods. Note that for the CS methods only 50% of the measurements were used. CS without SBT (Figure 6(c)) shows reduced image quality as compared to MF. By assuming a sparse range profile weak target returns are suppressed which is why the upper parts of the three letters can not be reconstructed anymore. CS with SBT as shown in Figure 6(d) on the other hand is able to accurately reconstruct the image and even shows a slight improvement in terms of image quality as compared to MF.

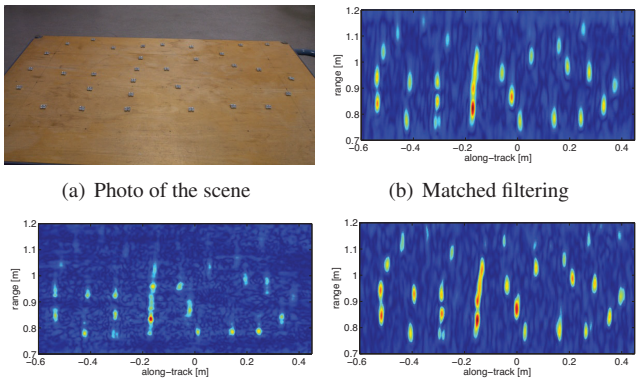

(a) Photo of the scene (b) Matched filtering

(c) CS without SBT (d) CS with SBT

Fig. 6. Imaging results

7. REFERENCES

[1] J.C. Jakowatz, D.E. Wahl, P.H. Eichel, D.C. Ghiglia, and P.A. Thompson, *Spotlight Mode Synthetic Aperture Radar: A Signal Processing Approach*, Kluwer, Boston, 1996.

[2] E. J. Candes and M. B. Wakin, "An introduction to compressive sampling," *IEEE Signal Processing Magazine*, vol. 25, no. 2, pp. 21–30, 2008.

[3] J. Romberg, "Imaging via compressive sampling," *IEEE Signal Processing Magazine*, vol. 25, no. 2, pp. 14–20, 2008.

[4] M. Leigsnering, C. Debes, and Abdelhak M. Zoubir, "Compressive sensing in through-the-wall radar imaging," in *Proc. IEEE Int Acoustics, Speech and Signal Processing (ICASSP) Conf*, 2011, pp. 4008–4011.

[5] M. Tello Alonso, P. Lopez-Dekker, and J. J. Mallorqui, "A novel strategy for radar imaging based on compressive sensing," *IEEE Transactions on Geoscience and Remote Sensing*, vol. 48, no. 12, pp. 4285–4295, 2010.

[6] M. Soumekh, *Synthetic Aperture Radar Signal Processing: with MATLAB Algorithms*, John Wiley & Sons, 1999.

[7] S. J. Wright, R. D. Nowak, and M. A. T. Figueiredo, "Sparse reconstruction by separable approximation," *IEEE Transactions on Signal Processing*, vol. 57, no. 7, pp. 2479–2493, 2009.